Journal of the Korean Institute of Illuminating and Electrical Installation Engineers (2014) 28(11) : 93~99
http://dx.doi.org/10.5207/JIEIE.2014.28.11.093 ISSN 1229-4691(Print) ISSN 2287-5034(Online)

논문 28-11-12

Application of the Method of Moments to the Capacitance Computation of a Parallel-Plate Rectangular Capacitor

Young-Su Roh*

Abstract

The method of moments is applied to numerically compute the electrostatic capacitance of a parallel-plate rectangular capacitor of finite area. Each plate is discretized into 900 patches per unit area to ensure a high accuracy of computation. To further enhance computational results, the impedance matrix elements are additionally evaluated in the case that the observation patch is located above or below the source patch in the vertical direction. To examine the fringing effect at the edges of the capacitor, the normalized capacitances are computed as a function of separation distance. After these results have been verified by Palmer's formula, this method is extended to the computation of capacitances between two different size plates.

Key Words : Method of Moments, Capacitance, Parallel-Plate Capacitor, Impedance Matrix, Fringing Effect

1. Introduction

The capacitance computation is an essential procedure in the design of conductor structures such as pulse forming lines [1] and long parallel transmission lines [2]. If the conductors are of an infinite extent such that symmetry conditions of the electric field exist, Gauss's law can be employed to find a uniform electric field between the conductors. Integrating the electric field makes it possible to obtain the electric potential difference. Under these assumptions, the capacitance of a parallel-plate capacitor C_0 can be expressed in the following analytic form [3].

$$C_0 = \frac{\varepsilon S}{D} \tag{1}$$

where ε is the permittivity of the medium, S is the plate area, and D is the separation distance between the two plates. Eq. (1) is valid as long as the separation distance is sufficiently smaller than the plate dimension. However, Eq. (1) does not provide an accurate value for the capacitance when the separation distance is large compared to the plate

* Main author : Soongsil University, Dept. of Electrical Engineering
Tel : 02-820-0663, Fax : 02-817-7961
E-mail : yroh@ssu.ac.kr
Date of submit : 2014. 8. 26
First assessment : 2014. 8. 29
Completion of assessment : 2014. 9. 11

width or length. In the case of a parallel-plate capacitor of finite area, for example, an analytic solution for the electric potential difference cannot be obtained using Gauss's law because the electric field lines are not uniform at the edges of the plates due to the fringing effect. Hence, it is necessary to numerically solve the electric potential.

Many numerical methods can be used to find the electric potential. These include the finite element method (FEM), finite difference method (FDM), boundary element method (BEM) and the method of moments (MoM). Like BEM, MoM solves the integral equation, while FEM and FDM solve the differential equation. Since MoM requires only the discretization of unknown functions, it does not suffer from numerical dispersion and the matrix size is smaller. Due to such conceptual and computational simplicity, MoM is suitable for the capacitance computation of a wire or plate structure [4-6]. For these reasons, MoM is used in this paper to compute the capacitances of parallel-plate rectangular capacitors.

The definition of the capacitance requires the net charge of the two plates to be zero. In MoM, this condition is satisfied if the dimensions of the two plates are equal. Therefore, there is no theoretical difficulty computing the capacitance. However, this condition is not satisfied if the dimensions are different. In the case of two cylindrical conductors of finite length, for instance, the total charges on the inner conductor are different from those on the outer conductor because the surface areas of the conductors are unequal [7]. In fact, this runs counter to the charge conservation law. Hence, it is difficult to compute capacitances between two different size plates using MoM. In this paper, this problem is solved by imposing the condition of zero total charge on the impedance matrix.

This paper is organized as follows. In Section 2, the basic theory of MoM is explained. In Section 3, the results of computations are discussed. To examine the fringing field effect, the surface charge distribution and the capacitances of the capacitor of the same plates are computed as the separation distance is changed. After these results are verified by Palmer's formula, a program developed based on MoM is applied to the computation of capacitances between two different size plates. Finally, the conclusion of the paper is presented.

2. Basic Theory

In a simple homogeneous medium, the electric potential is governed by Poisson's equation. An integral solution to Poisson's equation at an observation point $\boldsymbol{r}$, due to the charge density at a source point $\boldsymbol{r'}$ is given by [3]

$$V(\boldsymbol{r}) = \int \frac{\rho_v(\boldsymbol{r'})dv'}{4\pi\varepsilon|\boldsymbol{r}-\boldsymbol{r'}|} \tag{2}$$

where, ρ_v is the volume charge density. Consider a parallel-plate rectangular capacitor of width W, length L, and separation distance D. If charges reside only on its surfaces and the plate thickness can be neglected, Eq. (2) should be replaced by the following surface integral.

$$V(\boldsymbol{r}) = \int \frac{\rho_s(\boldsymbol{r'})ds'}{4\pi\varepsilon|\boldsymbol{r}-\boldsymbol{r'}|} \tag{3}$$

where, ρ_s is the surface charge density. If the electric potential is known, Eq. (3) is the integral equation for the unknown surface charge density. Namely, Eq. (3) makes it possible to find the surface charge distribution for a predefined electric potential difference between the two plates.

The potential on each plate is determined by

charges on its own plate and the other plate. If V_{11} (or V_{22}) is the potential on the upper (or lower) plate due to its own charge and V_{12} (or V_{21}) is the potential on the upper (or lower) plate due to the charge on the lower (or upper) plate, the potential V_1 (or V_2) on the upper (or lower) plate is given by

$$V_1 = V_{11} + V_{12}, \quad V_2 = V_{21} + V_{22} \tag{4}$$

In the Cartesian coordinate,

$$V_{11} = \frac{1}{4\pi\varepsilon} \int_{x'=0}^{W} \int_{y'=0}^{L} \frac{\rho_{1s} dx' dy'}{\sqrt{(x-x')^2 + (y-y')^2}} \tag{5}$$

$$V_{12} = \frac{1}{4\pi\varepsilon} \int_{x'=0}^{W} \int_{y'=0}^{L} \frac{\rho_{2s} dx' dy'}{\sqrt{(x-x')^2 + (y-y')^2 + D^2}} \tag{6}$$

$$V_{21} = \frac{1}{4\pi\varepsilon} \int_{x'=0}^{W} \int_{y'=0}^{L} \frac{\rho_{1s} dx' dy'}{\sqrt{(x-x')^2 + (y-y')^2 + D^2}} \tag{7}$$

$$V_{22} = \frac{1}{4\pi\varepsilon} \int_{x'=0}^{W} \int_{y'=0}^{L} \frac{\rho_{2s} dx' dy'}{\sqrt{(x-x')^2 + (y-y')^2}} \tag{8}$$

where ρ_{1s} and ρ_{2s} are surface charge densities on upper and lower plates, respectively. The procedure for applying MoM to equations (5-8) involves the following steps: (1) discretization of the equations into a matrix equation using pulse basis functions and weighting functions, (2) evaluation of the impedance matrix elements, (3) computation of the surface charge densities.

2.1 Discretization of the integral equations

To apply MoM to equations (5-8), the entire surfaces of the two plates are discretized into small rectangular patches [4]. The upper plate is equally divided into M segments along the x-direction, which are further divided into N segments along the y-direction. As a result, the upper plate is divided into MN rectangular patches of equal area. The lower plate is also divided into MN rectangular patches in the same way. The unknown surface charge densities are expressed in terms of MN basis functions with unknown coefficients α_n as [5]

$$\rho_{1s}(\mathrm{r}') = \sum_{n=1}^{MN} \alpha_n f_n(\mathrm{r}'), \quad \rho_{2s}(\mathrm{r}') = \sum_{n=NM+1}^{2MN} \alpha_n f_n(\mathrm{r}') \tag{9}$$

where ρ_{1s} and ρ_{2s} are charge densities on upper and lower plates, respectively. f_n is a set of pulse functions, i.e. $f_n = 1$ on the nth patch and $f_n = 0$ on any other patch. Substituting Eq. (9) into equations (5-8) and using point matching [5],

$$V_{11} = \sum_{n=1}^{MN} \alpha_n z_{mn}, \quad 1 \le m \le MN \tag{10}$$

$$V_{12} = \sum_{n=MN+1}^{2MN} \alpha_n z_{mn}, \quad 1 \le m \le MN \tag{11}$$

$$V_{21} = \sum_{n=1}^{MN} \alpha_n z_{mn}, \quad MN \le m \le 2MN \tag{12}$$

$$V_{22} = \sum_{n=MN+1}^{2MN} \alpha_n z_{mn}, \quad MN \le m \le 2MN \tag{13}$$

Using the above equations, Eq. (4) can be expressed in the following matrix equation.

$$[z_{mn}][\alpha_n] = [b_n] \tag{14}$$

Here $[z_{mn}]$ is a square matrix of the size of 2MN

×2MN. For convenience sake, this matrix is called the impedance matrix. $[\alpha_n]$ is a column matrix of the size of 2MN×1, which makes it possible to determine unknown charges on all rectangular patches. $[b_n]$ is also a column matrix of the size of 2MN×1, representing electric potentials. $b_n = V_1$ and V_2 for $1 \le m \le MN$ and $MN \le m \le 2MN$, respectively.

2.2 Evaluation of the impedance matrix elements

The impedance matrix elements are evaluated in the following three cases: (1) observation and source patches are different, (2) observation and source patches are identical, and (3) the observation patch is located above or below the source patch in the vertical direction.

In the first case, $z_{mn}(m \neq n)$ denotes the non-diagonal element of the impedance matrix, which is related to the electric potential at the center of observation patch m due to charges on the surface of source patch n. Note that observation and source patches can be on the same plate or different plates. If the two patches are on the same plate, the matrix element is expressed as follows.

$$z_{mn} = \frac{1}{4\pi\varepsilon} \int_{(n-1)\Delta x}^{n\Delta x} \int_{(n-1)\Delta y}^{n\Delta y} \frac{dx'dy'}{\sqrt{(x_m - x')^2 + (y_m - y')^2}} \quad (15)$$

where 1 ≤ m ≤ MN and 1 ≤ n ≤ MN, or MN+1 ≤ m ≤ 2MN and MN+1 ≤ n ≤ 2MN. Δx=W/M, Δy=L/N. If the two patches are on different plates, on the other hand,

$$z_{mn} = \frac{1}{4\pi\varepsilon} \times \int_{(n-1)\Delta x}^{\Delta x\Delta x} \int_{(n-1)\Delta y}^{n\Delta y} \frac{dx'dy'}{\sqrt{(x_m - x')^2 + (y_m - y')^2 + D^2}} \quad (16)$$

where 1 ≤ m ≤ MN and MN+1 ≤ n ≤ 2MN, or MN+1 ≤ m ≤ 2MN and 1 ≤ n ≤ MN. Since it is time-consuming to directly integrate equations (15-16) for all rectangular patches, these matrix elements are computed using a central-point approximation: observation and source points are placed at the centers of patches m and n [6]. In this approximation, equations (15-16) are rewritten as

$$z_{mn} = \frac{1}{4\pi\varepsilon} \frac{\Delta x\Delta y}{\sqrt{(x_m - x_n)^2 + (y_m - y_n)^2}} \quad (17)$$

$$z_{mn} = \frac{1}{4\pi\varepsilon} \frac{\Delta x\Delta y}{\sqrt{(x_m - x_n)^2 + (y_m - y_n)^2 + D^2}} \quad (18)$$

In the second case, $z_{nn}(m = n)$ is the diagonal element that corresponds to the electric potential at the center of patch n due to charges on its own surface. At the center of patch n,

$$z_{nn} = \frac{1}{4\pi\varepsilon} \int_{-\Delta x/2}^{\Delta x/2} \int_{-\Delta y/2}^{\Delta y/2} \frac{dx'dy'}{\sqrt{x'^2 + y'^2}} \quad (19)$$

Using the following integral formula with integration constant k [8],

$$\int \frac{dx}{\sqrt{x^2 + y^2}} = \ln\left(x + \sqrt{x^2 + y^2}\right) + k \quad (20)$$

Eq. (19) can be expressed in a simple algebraic form:

$$z_{nn} = \frac{1}{4\pi\varepsilon} \left\{ \begin{array}{l} \Delta x \ln\left(\frac{\sqrt{\Delta x^2 + \Delta y^2} + \Delta y}{\sqrt{\Delta x^2 + \Delta y^2} - \Delta y}\right) + \\ \Delta y \ln\frac{\Delta x\left(\sqrt{\Delta x^2 + \Delta y^2} + 2\Delta x\right) + \Delta y^2}{\Delta y^2} \end{array} \right\} \quad (21)$$

In the last case, $z_{mn}(n = m \pm MN)$ represents the

elements that correspond to the potential at the center of observation patch m of the upper (or lower) plate due to charges on source patch n of the lower (or upper) plate along the z-direction. At the center of patch m,

$$z_{mn} = \frac{1}{4\pi\varepsilon} \int_{-\Delta x/2}^{\Delta x/2} \int_{-\Delta y/2}^{\Delta y/2} \frac{dx'\,dy'}{\sqrt{x'^2+y'^2+D^2}} \tag{22}$$

Applying appropriate integral formulas to Eq. (22),

$$z_{mn} = \Delta y \ln \frac{K+\Delta x}{K-\Delta x} + \Delta x \ln \frac{K+\Delta y}{K-\Delta y} - 4D \tan^{-1} \frac{\Delta x \Delta y}{2DK} \tag{23}$$

where $K = \sqrt{\Delta x^2 + \Delta y^2 + 4D^2}$. The total charges on the upper plate are computed as follows.

$$Q = \sum_{n=1}^{MN} \sum_{n=1}^{MN} \alpha_n \frac{WL}{MN} \tag{24}$$

3. Results of Numerical Computation

A MATLAB program was developed based on equations (17), (18), (21), and (23). Before computing the capacitance, it is important to decide the number of patches to ensure a high computational accuracy. Fig. 1 depicts how the normalized capacitance (C/C_0) changes as the number of patches increases. These results can be obtained using the capacitor of W=1m, L=1m and $\varepsilon = \varepsilon_0$ under the assumption that potentials on upper and lower plates are 1V and -1V, respectively. The capacitance increases abruptly as the number of patches increases up to 100 regardless of the separation distance. After 100 patches, it increases gradually and converges to a constant value. Hence, the number of patches per unit area is chosen to be 900(M=N=30).

Fig. 2 illustrates the surface charge distributions obtained with the capacitor of W=1m, L=0.5m, D=0.5m and $\varepsilon = \varepsilon_0$. The charge accumulates near the corners and the edges of the plates due to the fringing effect.

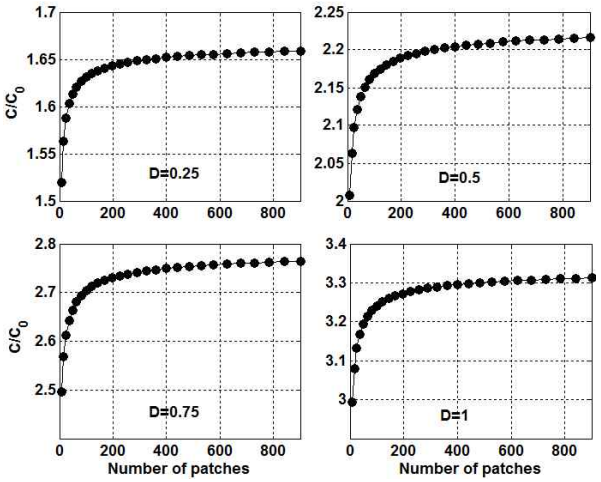

Fig. 1. Plots of the normalized capacitance as a function of the number of patches

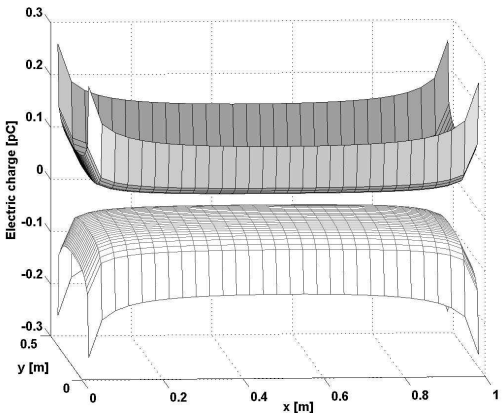

Fig. 2. Surface charge distributions on the plates

Fig. 3 shows computed capacitances of the capacitor of W=1m, L=1m and $\varepsilon = \varepsilon_0$. It can be observed that C is always larger than C_0. This is

expected due to the fringing effect. To quantitatively analyze the fringing effect, the normalized capacitance is plotted as a function of separation distance as shown in Fig. 4. As can be seen, the normalized capacitance is directly proportional to the separation distance when $D > 0.1$ m. Note that a bigger value of the normalized capacitance indicates a greater effect of the fringing field. The fringing effect increases linearly as the separation distance increases. However, it is negligible as the separation distance approaches zero.

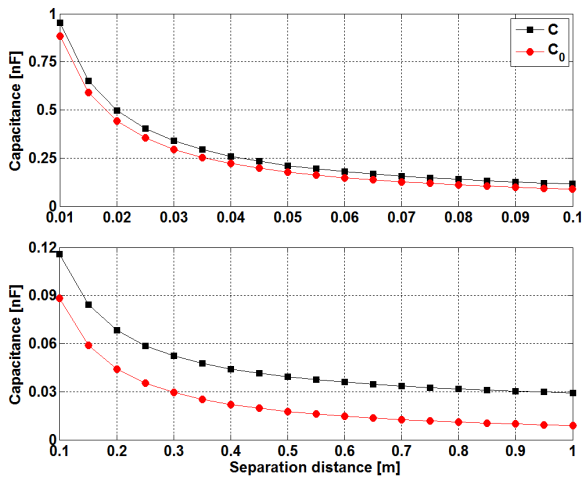

Fig. 3. Plot of capacitance versus separation distance

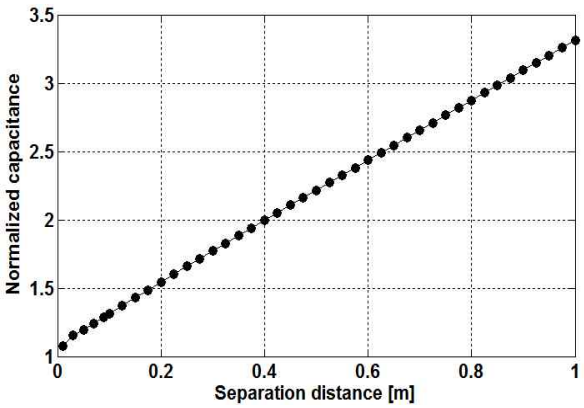

Fig. 4. Plot of normalized capacitance versus separation distance

To confirm the simulation results of MoM, they are compared to Palmer's formula, which is derived based on the conformal mapping transformation. This formula is expressed as follows [9-10].

$$C = \frac{\varepsilon WL}{D}\left(1+\frac{D}{\pi W}+\frac{D}{\pi W}\ln\frac{2\pi W}{D}\right) \times\left(1+\frac{D}{\pi L}+\frac{D}{\pi L}\ln\frac{2\pi L}{D}\right) \quad (25)$$

Fig. 5 displays the plots of capacitances obtained using MoM and Palmer's formula. MoM shows an excellent agreement with Palmer's formula. Since its computational performance is confirmed, the MoM program can be applied to the capacitance computation of the capacitor between two different size plates. In this case, the condition of the net electric charge equal to zero is not satisfied in Eq. (14). [11] suggested a method to enforce this condition as follows: Divide each row of Eq. (14) by the corresponding rectangular area, then subtract the last row of Eq. (14) from the others, and replace this last equation by the charge conservation law. This scheme is applied to compute capacitances between two different size plates. An example is shown in Fig. 6. Here, the length and the width of

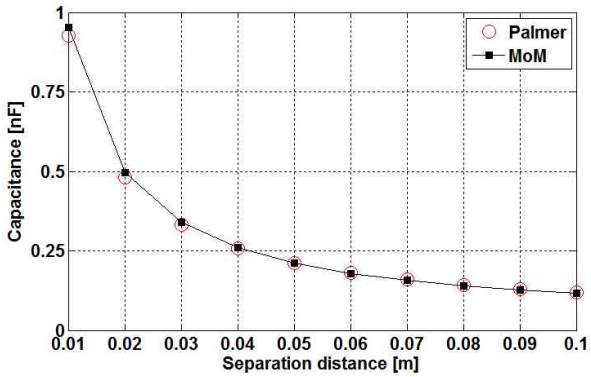

Fig. 5. Comparison between the method of moments and Palmer's formula

the upper plate are fixed at a value of 1m. The length of the lower plate is also 1m, while the width of the lower plate is chosen to be a variable. As can be seen, the capacitance converges after the width of the lower plate approaches 4m.

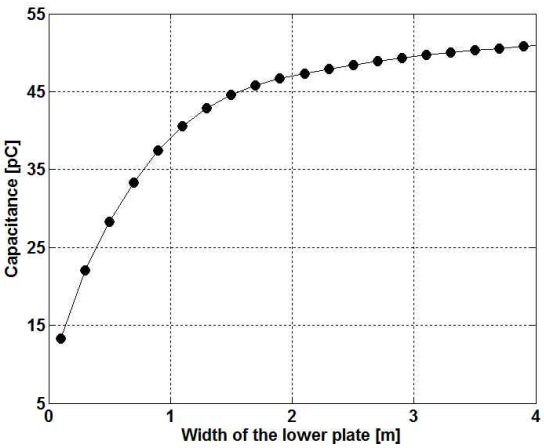

Fig. 6. Capacitance between two different size plates as a function of the width of the lower plate

4. Conclusion

MoM was applied to find the surface charge density distribution and the capacitance of a parallel-plate rectangular capacitor of finite area. It was found that the fringing effect becomes stronger as the separation distance increases. It was verified by the excellent agreement between MoM and the Palmer's formula that MoM is capable of solving the integral equation for the charge density. It was also proved by the computation results of the capacitance between two different size plates that the charge conservation law is successfully imposed on the MoM matrix equation.

References

[1] Y. Roh and Y. S. Jin, "Analysis of Output Pulse of High Voltage and Nanosecond Blumlein Pulse Generator," J. Electr. Eng. Technol., Vol. 8, No. 1, pp. 150-155, 2013

[2] C. R. Paul, "Analysis of Multi-conductor Transmission Lines," John Wiley and Sons Inc., 2008.

[3] D. K. Cheng, "Fundamentals of Engineering Electromagnetics," Addison-Wesley Publishing Company, Inc., 1993.

[4] R. F. Harrington, "Field Computation by Moment Methods," Macmillan, New York, 1968.

[5] W. C. Gibson, "The Method of Moments in Electromagnetics," Chapman & Hall/CRC, 2008.

[6] M. N. O. Sadiku, "Numerical Techniques in Electromagnetics," CRC Press LLC, 2001.

[7] N. S. Das and S. B. Chakrabarty, "Capacitance and charge distribution of two cylindrical conductors of finite length," IEE, Proc. Sci. Meas. Technol. Vol. 144, No. 6, pp. 280 - 286, 1997.

[8] www.wolframalpha.com

[9] B. Palmer, "Capacitance of a parallel-plate capacitor by the Schwartz-Christoffel transformation," Transactions on AIEE, Vol. 56, No. 3, pp. 363 - 366, 1937.

[10] M. Hosseini, G. Zhu and Y. Peter, "A new formulation of fringing capacitance and its application to the control of parallel-plate electrostatic micro actuators," Analog Integr. Circ. Sig. Process, Vol. 53, pp. 119-128, 2007.

[11] M. B. Bazdar, A. R. Djordjevic, R. G. Harrington, and T. K. Sarkar, "Evaluation of quasi-static matrix parameters for multiconductor transmission lines using Galerkin's method," IEEE Trans. Microwave Theory Tech., Vol. 47, No. 7, pp. 1223-1228, 1994.

Biography

Young-Su Roh

Young-Su Roh received his B.S. and M.S. degrees in Electrical Engineering from Seoul National University in 1984 and 1986, respectively. He received a Ph.D. degree in Applied Science from the University of California, Davis in 2001. From 1988 to 1996, he worked at the Korea Electricity Research Institute. He is now an associate professor of the Department of Electrical Engineering at Soongsil University. His research fields are plasma physics, nuclear fusion, and electrical discharges.